Letter

Adiabaticity enhancement in the classical transverse field Ising chain, and its effective non-Hermitian description

Balázs Dóra[1,2,*] and Roderich Moessner[3]

[1]*MTA-BME Lendület Topology and Correlation Research Group, Budapest University of Technology and Economics, Műegyetem rakpart 3, H-1111 Budapest, Hungary*

[2]*Department of Theoretical Physics, Institute of Physics, Budapest University of Technology and Economics, Műegyetem rakpart 3, H-1111 Budapest, Hungary*

[3]*Max-Planck-Institut für Physik komplexer Systeme, D-01187 Dresden, Germany*

(Received 15 March 2023; accepted 16 August 2023; published 7 September 2023)

We analyze the near-adiabatic dynamics in a ramp through the critical point (CP) of the classical transverse field Ising chain. This is motivated, conceptually, by the fact that this CP—unlike its quantum counterpart—experiences no thermal or quantum fluctuations, and technically by the tractability of its effective model. For a "half ramp" from a ferromagnet to the CP, the longitudinal and transverse magnetizations scale as $\tau^{-1/3}$ and $\tau^{-2/3}$, respectively, with $1/\tau$ the ramp rate, in accord with Kibble-Zurek theory. For ferro- to paramagnetic ramps across the CP, however, they stay closer, $\tau^{-1/2}$ and τ^{-1}, to adiabaticity. This adiabaticity enhancement compared to the half ramp is understood by casting the dynamics in the paramagnet in the form of a non-Hermitian Dirac Hamiltonian, with the CP playing the role of an exceptional point, opening an additional decay channel.

DOI: 10.1103/PhysRevB.108.L121105

Introduction. Recently, the study of the nonequilibrium dynamics of many-body systems has attracted enormous interest [1,2]. In particular, defect production after the nonadiabatic passage through a critical point was found to exhibit universal behavior with a scaling that is determined solely by the universality class of the underlying phase transition [3,4]. This, the celebrated Kibble-Zurek mechanism, has been most directly verified in the transverse field Ising chain [5,6].

Indeed, the transverse field quantum Ising chain [7] is a paradigmatic, and one of the most thoroughly studied, models in physics. It plays an important role in understanding quantum phase transitions [8] and duality, conformal field theory [9], and is relevant, through a quantum to classical mapping, for the statistical mechanics of the classical Ising model in two dimensions. Moreover, it is closely tied to topological phenomena [10] and the Kitaev chain [11]. In addition to its theoretical appeal, experimental realizations involve condensed [12,13] and artificial [14] matter.

Surprisingly, despite the great amount of interest in the transverse field quantum Ising chain, its classical counterpart has received only limited attention. This is all the more remarkable as the study of classical spin chains has unearthed a number of surprises [15,16], such as a regime of Kardar-Parisi-Zhang scaling in the Heisenberg chain [17] or generalized hydrodynamics [18]. Moreover, classical spin models are ubiquitous in that they are widely used not only in physics [8,19,20], but also to model complex systems such as neural or social networks [21], and physical realizations include large interacting quantum spins [20], polariton simulators [22], coupled nanolaser lattices [23], cold atoms with total collective spin dynamics [24], or precessing rigid bodies such as a spinning top [25].

The identical ground state phase diagrams [8,26,27] of classical and quantum transverse field Ising chains, being nonintegrable [28] and integrable [8], respectively, possess ferromagnetic (FM) and paramagnetic (PM) phases, separated by a critical point (CP). However, critical exponents and the ensuing universality classes are distinct. Moreover, the classical version lacks both quantum and thermal fluctuations, rendering the corresponding CP unusual.

Here, we investigate the nonequilibrium dynamics in the classical transverse field Ising chain for a wide variety of ramps, starting from a ground state. We summarize the scaling of physical quantities with the ramp speed in Table I. While many decay exponents are in accord with Kibble-Zurek scaling, those of deviations of the spins from adiabaticity for a ramp from the FM across the CP differ—*they stay closer to the adiabatic limit.* Our analysis accounts for this by interpreting the classical dynamics as a non-Hermitian Dirac Hamiltonian, where the CP plays the role of an exceptional point, which allows for an additional decay channel due to effective nonunitary dynamics.

We study the one-dimensional Hamiltonian

$$H = \sum_n -JS_n^x S_{n+1}^x - 2gS_n^z, \tag{1}$$

with unit length classical spins $\mathbf{S}_n \in S^2$ and ferromagnetic Ising coupling $J = 1$, and transverse field strength $g > 0$. We use periodic boundary conditions for the N spins. For $g < 1$, the ground state is FM [26,30] and $S_{n,\mathrm{gs}}^x = \pm\sqrt{1-g^2}$, $S_n^z = g$, the $\pm$ signs corresponds to the two degenerate ground state configurations. The ground state energy per spin is

*dora.balazs@ttk.bme.hu

TABLE I. The exponent of deviations from the adiabatic value for several physical quantities as τ^{-a} for various ramps. For the PM to FM ramp, no defects are created. The PM initial state $\mathbf{S}_n = (0, 0, 1)$ remains the solution of the Landau-Lifshitz equation for any time-dependent $g(t)$. The FM to FM ramp is unrelated to Kibble-Zurek theory since no CP is crossed. The scaling of the excess energy as well as the FM to CP ramp follow the Kibble-Zurek theory. The bold exponents follow from an effective non-Hermitian dynamics. These exponents survive moderate randomness [29] in the initial spin configuration.

	Observables			
Ramp type	$\delta^x(\tau)$	$\delta^y(\tau)$	$\delta^z(\tau)$	$\Delta E(\tau)/N$
FM → FM	1	1	1	2
FM → CP	1/3	2/3	2/3	4/3
FM → PM	**1/2**	**1/2**	**1**	1

$E_{\rm gs}/N = -2g - (1-g)^2$. In the PM, $S^z_{n,\rm gs} = 1$ for $g > 1$ with ground state energy $E_{\rm gs}/N = -2g$. These two regions are separated by a classical CP at $g = 1$, which corresponds to a continuous second-order classical phase transition upon tuning the transverse field with critical exponents $\alpha = 0$, $\beta = 1/2$, without thermal or quantum fluctuations at zero temperature. The nonanalytic behavior of the transverse magnetization at $g = 1$ also allows us to define the corresponding critical exponent $\beta_z = 1$.

The spin dynamics of the model is obtained from the classical Landau-Lifshitz equation of motion

$$\partial_t \mathbf{S}_n = \mathbf{B}_n \times \mathbf{S}_n, \tag{2}$$

where the effective magnetic field for the nth spin is

$$\mathbf{B}_n = -\big(S^x_{n-1} + S^x_{n+1}, 0, 2g\big). \tag{3}$$

A classical linear spin-wave theory [19] analysis reveals that in the PM, the energy spectrum is $\omega_q = 2\sqrt{g[g - \cos(q)]}$ with q the momentum. The energy disperses linearly with momentum around $q = 0$ at the CP $g = 1$, giving the dynamical critical exponent $z = 1$, while the gap collapses as $\sim\sqrt{g-1}$ upon approaching the critical point [30], defining the exponent of the correlation length as $\nu = 1/2$. In the FM, the spin-wave spectrum is $\omega_q = 2\sqrt{1 - g^2\cos(q)}$, yielding the same ν and z. During any nonequilibrium dynamics, the system heats up, and thermal fluctuations appear.

Similarly to its quantum counterpart [1,2,5,6], we are interested in ramping the transverse field as $g(t) = g_0 + (g - g_0)t/\tau$ across the classical CP with a speed of $1/\tau$ and $0 < t < \tau$. Since these ramps are spatially homogeneous and start from the ground state, where all spins behave identically, the dynamics involves only the homogeneous long-wavelength ($q = 0$) mode of the spins, and it suffices to study the dynamics of a single spin as

$$\partial_t \mathbf{S} = \mathbf{B} \times \mathbf{S} \quad \text{with } \mathbf{B} = -2(S^x, 0, g). \tag{4}$$

This corresponds to the effective Hamiltonian [30]

$$H = -(S^x)^2 - 2gS^z \tag{5}$$

of a single classical spin with uniaxial anisotropy in the presence of transverse field. Note that this applies to spatially homogeneous quenches in the ground states of the classical model in Eq. (1). The spatial correlation length is infinite in the original model and loses its meaning in the effective description, where only temporal fluctuations appear. This simplifies the problem immensely since only three, rather than $3N$, coupled differential equations need to be solved. We have also investigated the full lattice model numerically in the Supplemental Material [29] (see also Refs. [31–33] therein) and found identical results to the single-spin model. Dynamics in the quantum version of Eqs. (1) and (5) was considered in Refs. [5,6,34–38].

Ramp from PM. For quenches with $g_0 > 1$ and any final g, the initial spin configuration, $\mathbf{S} = (0, 0, 1)$, is stationary and remains a solution of Eq. (4) for any time-dependent transverse field, in contrast to the Kibble-Zurek mechanism [3,4,39], where the final energy density depends on the ramp rate. Here, it is determined by the energy of the infinitely long-lived "scar state." Loosely speaking, the system can neither choose any spin configuration (up or down in the x direction) on the FM side for a spatially homogeneous quench, nor can it be in a superposition due to the classical nature of the spins. The same applies to ramps starting from the ground state at the CP.

Ramp within the FM phase. For simplicity, we consider $g(t) = gt/\tau$ with $0 < t < \tau$ and $g < 1$. By introducing the difference

$$\delta^j(t) = S^j(t) - S^j_{\rm gs}[g(t)], \quad j = x, y, z, \tag{6}$$

between the time-evolved and adiabatic ground state values of the spins, the effective dynamics to lowest order in δ is described from Eq. (4) by only two coupled equations as

$$\partial_t \delta^y(t) = 2\sqrt{1 - (gt/\tau)^2}\,\delta^z(t), \tag{7a}$$

$$\partial_t \delta_z(t) = -2\sqrt{1 - (gt/\tau)^2}\,\delta_y(t) - \frac{g}{\tau}, \tag{7b}$$

with initial condition $\delta^{y,z}(t = 0) = 0$ and $S^x(t)$ implicit via the unit length constraint. For $g \ll 1$ and long enough quenches, this is solved to a good approximation by taking $\sqrt{1 - (gt/\tau)^2}$ as a time-independent constant to yield

$$\delta^z(t) = -\frac{g \sin\left[2\int_0^t \sqrt{1 - (gt'/\tau)^2}\,dt'\right]}{2\tau\sqrt{1 - (gt/\tau)^2}}, \tag{8}$$

and $\delta^y(t)$ follows from using Eq. (7b). Notably, both contain the $1/\tau$ term from the denominator of Eq. (8), which stems from the source term in Eq. (7b). At the end of the quench $t = \tau$, all spin components deviate from their ground state values $\sim\tau^{-1}$. From this and Eq. (5), the naive expectation for the scaling of the excess energy would be the same. However, in reality, the excess energy vanishes as τ^{-2} since the τ^{-1} prefactors in the two terms in Eq. (5) cancel. This is expected to be the typical scaling for the near-adiabatic dynamics away from the CP [40].

Ramp from FM to CP. In this case, we consider $g(t) = t/\tau$ with $0 < t < \tau$. The dynamics is still described by Eq. (7) with $g = 1$, and the time evolution ends at the CP. From a numerical analysis of the problem, we learn that to a good approximation, $\sqrt{1 - [S^x(t)]^2} \approx S^z(t) = \frac{t}{\tau} + \delta^z(t)$.

At the heart of the problem lies the square root vanishing longitudinal spin component, $\sqrt{1 - (t/\tau)^2}$ at the CP, which

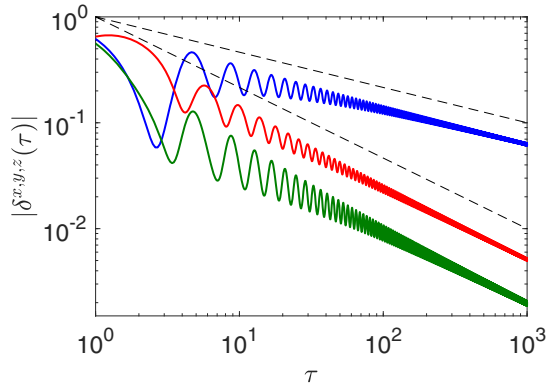

FIG. 1. Numerical data for deviations from the adiabatic value for spin components x, y, and z (blue, red, and green) from top to bottom after quenching to the critical point ($g = 1$) from the FM ($g_0 = 0$) phase. The black dashed lines depict the $\tau^{-1/3}$ and $\tau^{-2/3}$ scalings.

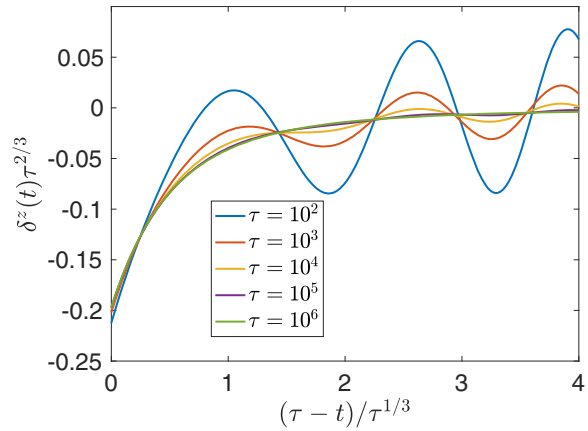

FIG. 2. Temporal data collapse of $\delta^z(t)$ close to the CP for various ramp rates after a ramp from the FM ($g_0 = 0$). The data are obtained from the numerical solution of Eq. (4). Deviations from zero start to appear at times $\sim\tau^{1/3}$ before reaching the CP. A similar data collapse characterizes the other spin components.

renders any adiabatic approximation rather difficult, since any temporal derivative of the above expression diverges at the CP. This can be cured by retaining higher-order terms in δ in Eq. (7). In this case, we have to replace the $\sqrt{1-(t/\tau)^2}$ term by $\sqrt{1-[t/\tau+\delta^z(t)]^2}$ which cures the aforementioned singularity at the CP for any finite $\delta^z(\tau)$. Equation (8) is replaced by

$$\delta^z(t) = -\frac{\sin[2\phi(t)]}{2\tau\sqrt{1-[t/\tau+\delta^z(t)]^2}}, \tag{9}$$

with $\phi(t) = \int_0^t \sqrt{1-[t'/\tau+\delta^z(t')]^2}dt'$. The self-consistency condition at the end of the quench at the CP reads

$$\delta^z(\tau) \approx -\frac{\sin[2\phi(\tau)]}{2\tau\sqrt{-2\delta^z(\tau)}}, \tag{10}$$

which yields $\delta^z(\tau) \sim \tau^{-2/3}$ and $\delta^y(\tau)$ follows the same scaling via Eq. (7b). From the unit length constraint, we obtain $\delta^x(\tau) \sim \tau^{-1/3}$. These features are shown in Fig. 1 from the full numerical solution of Eq. (4) using a fifth-order Runge-Kutta method.

The transition time $t_{\rm tr}$ when this scaling appears due to the close vicinity of the CP, is determined from $S^x(\tau - t_{\rm tr}) \approx 0$. Using the above scalings, this gives $t_{\rm tr} \sim \tau^{1/3}$: The presence of criticality makes its presence felt at $t \sim \tau - \tau^{1/3}$. These features are illustrated in Fig. 2. From the above scalings and the structure of the effective Hamiltonian in Eq. (5), it is tempting to conclude that the excess energy pumped into the system by the nonequilibrium ramp scales as $\Delta E/N \sim \tau^{-2/3}$, since both terms in Eq. (5) produce this scaling. This is, however, again not correct. The prefactors of the leading-order terms cancel, leaving the subleading term for the excess energy, $\Delta E/N \sim \tau^{-4/3}$.

These exponents follow Kibble-Zurek scaling [3,4]. In general, an operator is expected to scale with the speed of the drive after the ramp as [34,36,39,41] $O - O_0 \sim \tau^{-\chi/(1+\mu)}$ measured from its adiabatic value O_0 with χ the critical exponent associated to O and $\mu = z\nu$ in conventional Kibble-Zurek theory. Using the critical exponents for Eq. (1) for the spins and linear spin-wave theory, we obtain $\mu = 1/2$, the conventional value expected in related models [35,36]. Also the transition time [6] is expected to scale as $\tau^{\mu/(1+\mu)}$, in accord with Fig. 2. As to the excess energy, its critical exponent is [42] $2 - \alpha = 2$, which gives the observed $-4/3$ exponent. Note that these differ from those identified for the quantum counterparts [6,35,36] of Eqs. (1) and (5).

Ramp from FM to PM. This is the continuation of the previous FM to CP ramp. The temporal variation of the transverse field is $g(t) = gt/\tau$ with $g > 1$, $0 < t < \tau$. For the initial FM part of the ramp for $t < \tau/g$, we use the results in the previous section and pick up the time evolution at the critical point, $t = \tau/g$.

By linearizing Eq. (4), the effective dynamics couples only the x and y components, resulting in two coupled differential equations. These *equations of motion* may be written in a suggestive form of a non-Hermitian *Hamiltonian*, namely a Schrödinger equation [43–51] of a quantum spin-1/2 in a complex magnetic field or the non-Hermitian $(0+1)$-dimensional Dirac equation [52]

$$i\partial_t \begin{pmatrix} \delta^x(t) \\ \delta^y(t) \end{pmatrix} = \begin{pmatrix} 0 & 2ig(t) \\ -2ig(t)+2i & 0 \end{pmatrix} \begin{pmatrix} \delta^x(t) \\ \delta^y(t) \end{pmatrix}, \tag{11}$$

and $\delta^z(t)$ follows from the unit length spin constraint, $\tau/g < t < \tau$. Equation (11) is a non-Hermitian, parity-time ($\mathcal{PT}$)-symmetric [53–55] Dirac equation, where non-Hermiticity arises from the $2i\delta^x(t)$ term in Eq. (11). The instantaneous eigenvalues are $\pm 2\sqrt{g(t)[g(t)-1]}$. These vanish exactly at the CP $g(t) = 1$, $t = \tau/g$, where the effective dynamics starts. This corresponds to an exceptional point [48,49,56] with a vanishing spectrum at $g = 1$, consistent with the critical exponent $\mu = 1/2$. There, not only do the eigenvalues become degenerate but also the two *eigenstates* coalesce and no longer form a complete basis. The system becomes increasingly Hermitian with time for $g \gg 1$. The initial condition to Eq. (11) is the one and only eigenstate of the right-hand side of Eq. (11) at the exceptional point, namely $[\delta^x(\tau/g), \delta^y(\tau/g)] \sim \tau^{-1/3}(1, 0)$ [57].

This represents a variation of the theme of non-Hermitian Kibble-Zurek scaling [58,59]. By starting the time evolution from the single eigenstate of the Dirac equation in Eq. (11) at the exceptional point, the norm of the "wave function," $[\delta^x(t), \delta^y(t)]$ decays in time [60]. This occurs even in $\mathcal{PT}$-symmetric systems due to the nonunitary noneigenstate evolution. By taking a fixed $g(t) = g \gtrsim 1$ in Eq. (11), the norm of the initial state $(1, 0)$ evolves in time as $1 - g^{-1}\sin^2(Et)$ with $E = 2\sqrt{g(g-1)}$, which decays initially before revival sets in. However, by reintroducing $g(t)$, when the driving rate $\partial_t E/E$ is larger than the revival frequency E, there is not enough time for revival and only the norm decay remains. Most of the decay occurs at the close vicinity [58] of the exceptional point, i.e., within a $\tau^{1/3}$ temporal window, similarly to the FM side of the transition (see Fig. 2). The resulting suppression of $[\delta^x(\tau)]^2 + [\delta^y(\tau)]^2$ from its initial value scales as $\tau^{-1/3}$. This comes from $1/3 = \mu/(1+\mu)$. Altogether, the overall decay exponent of $\delta^x(\tau)$, including the initial value, is $1/2 = 1/3 + 1/6$. This is a combination of two factors: The $1/3$ comes from the $\tau^{-1/3}$ scaling of the initial condition, while the additional suppression factor $1/6$ from the non-Hermitian time evolution around the exceptional point, i.e., $\frac{1}{2}\mu/(1+\mu)$.

In addition to these scaling ideas, we treat these two coupled first-order differential equations with the Wentzel-Kramers-Brillouin (WKB) method, similarly to Dirac systems [61]. By solving the wave function away from the exceptional point, corresponding to the turning point in WKB approaches, we obtain the asymptotic form of the wave function. We then match this form with the initial exact solution of the linearized version of Eq. (11). This amounts to replacing $g(t)$ by g in the first line of Eq. (11) while keeping $g(t) = gt/\tau$ in the second line. This is solved exactly using Airy functions and we obtain $\delta^x(\tau) \sim \delta^y(\tau) \sim \exp[\pm i\tau 2\int_0^{g-1}\sqrt{t'(t'+1)}dt']\tau^{-1/2}$. The numerical solution of Eq. (4) using the Runge-Kutta method for the FM to PM ramp is illustrated in Fig. 3.

The deviation of the z component from the adiabatic value follows from the unit length constraint as $\delta^z(\tau) \sim [\delta^x(\tau)]^2 + [\delta^y(\tau)]^2 \sim \tau^{-1}$, i.e., the initial value $\sim\tau^{-2/3}$ is further suppressed by $\tau^{-\mu/(1+\mu)}$. Building on these, the excess energy also scales as τ^{-1}. This is connected to Kibble-Zurek ideas [62]: The difference between the $1/\tau$ exponent of excess energy for a half ramp and a full ramp is exactly $\mu/(1+\mu) = 1/3$, which translates to $4/3 - 1/3 = 1$ in our case.

Overall, the deviations from the adiabatic value of the spin are suppressed for a full FM $\to$ PM ramp compared to a half ramp. This chimes with the robustness of the PM ground state spin configuration, which remains immune to any quenches. But it is in contrast to the response of the quantum transverse field Ising chain, where the transverse magnetization follows the same $\tau^{-1/2}$ scaling for both full and half ramps [63,64].

Discussion. We have studied near-adiabatic dynamics in the classical transverse field Ising chain. Rich behavior and scaling are identified based on the ramp type, summarized in Table I. The scaling of physical quantities after the FM to CP ramp follows the Kibble-Zurek prediction. Most interestingly, the dynamics of the FM to PM ramp encompasses a region where the effective dynamics is described by a non-Hermitian Hamiltonian around an exceptional point, emerging from the classical equations of motion of the parent model. This effective non-Hermitian description incorporates a suppression of the defect production, accounting for the suppressed deviation from adiabaticity compared to the half ramp.

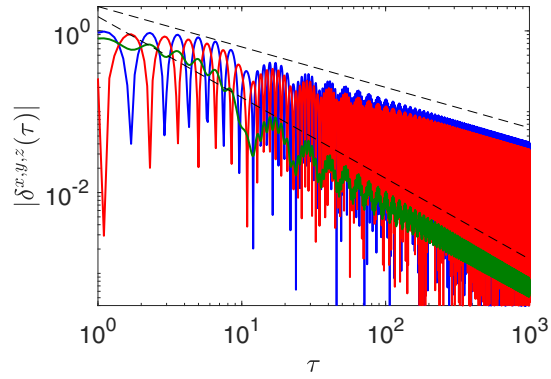

FIG. 3. Numerical solution of the deviations from the adiabatic value for spin components x, y, and z (blue, red, and green) from top to bottom after quenching from FM ($g_0 = 0$) to PM ($g = 3$). The black dashed lines depict the $\tau^{-1/2}$ and τ^{-1} scalings obtained analytically.

These results are not limited to the one-dimensional classical transverse field Ising model, but apply more generally. By considering $H = \sum_{\langle n,m\rangle} -JS_n^xS_m^x - gS_n^z$ for any lattice with uniform coordination in arbitrary dimensions, the very same phase diagram and effective Hamiltonian apply not only to the ground state properties but also for the near-adiabatic dynamics.

Acknowledgments. Useful discussions with M. Kormos and G. Takács are gratefully acknowledged. This research was supported by the Ministry of Culture and Innovation and the National Research, Development and Innovation Office within the Quantum Information National Laboratory of Hungary (Grant No. 2022-2.1.1-NL-2022-00004) K134437, K142179, and by a grant of the Ministry of Research, Innovation and Digitization, CNCS/CCCDI-UEFISCDI, under Project No. PN-III-P4-ID-PCE-2020-0277. This work was supported in part by the Deutsche Forschungsgemeinschaft under grants cluster of excellence ct.qmat (EXC 2147, Project-Id 390858490). This work was performed in part at Aspen Center for Physics, which is supported by National Science Foundation Grant No. PHY-2210452, and was also partially supported by a grant from the Simons Foundation.

[1] A. Polkovnikov, K. Sengupta, A. Silva, and M. Vengalattore, Colloquium: Nonequilibrium dynamics of closed interacting quantum systems, Rev. Mod. Phys. **83**, 863 (2011).

[2] J. Dziarmaga, Dynamics of a quantum phase transition and relaxation to a steady state, Adv. Phys. **59**, 1063 (2010).

[3] T. W. B. Kibble, Topology of cosmic domains and strings, J. Phys. A: Math. Gen. **9**, 1387 (1976).

[4] W. H. Zurek, Cosmological experiments in superfluid helium? Nature (London) **317**, 505 (1985).

[5] W. H. Zurek, U. Dorner, and P. Zoller, Dynamics of a Quantum Phase Transition, Phys. Rev. Lett. **95**, 105701 (2005).

[6] J. Dziarmaga, Dynamics of a Quantum Phase Transition: Exact Solution of the Quantum Ising Model, Phys. Rev. Lett. **95**, 245701 (2005).

[7] R. J. Elliott, P. Pfeuty, and C. Wood, Ising Model with a Transverse Field, Phys. Rev. Lett. **25**, 443 (1970).

[8] S. Sachdev, *Quantum Phase Transitions* (Cambridge University Press, Cambridge, UK, 1999).

[9] G. Mussardo, *Statistical Field Theory: An Introduction to Exactly Solved Models in Statistical Physics*, 1st ed., Oxford Graduate Texts (Oxford University Press, New York, 2010).

[10] A. Kitaev and C. Laumann, Topological phases and quantum computation, arXiv:0904.2771.

[11] A. Y. Kitaev, Unpaired Majorana fermions in quantum wires, Phys. Usp. **44**, 131 (2001).

[12] D. Bitko, T. F. Rosenbaum, and G. Aeppli, Quantum Critical Behavior for a Model Magnet, Phys. Rev. Lett. **77**, 940 (1996).

[13] A. W. Kinross, M. Fu, T. J. Munsie, H. A. Dabkowska, G. M. Luke, S. Sachdev, and T. Imai, Evolution of Quantum Fluctuations Near the Quantum Critical Point of the Transverse Field Ising Chain System $CoNb_2O_6$, Phys. Rev. X **4**, 031008 (2014).

[14] A. Keesling, A. Omran, H. Levine, H. Bernien, H. Pichler, S. Choi, R. Samajdar, S. Schwartz, P. Silvi, S. Sachdev, P. Zoller, M. Endres *et al.*, Quantum Kibble-Zurek mechanism and critical dynamics on a programmable Rydberg simulator, Nature (London) **568**, 207 (2019).

[15] R. W. Gerling and D. P. Landau, Comment on Anomalous Spin Diffusion in Classical Heisenberg Magnets, Phys. Rev. Lett. **63**, 812 (1989).

[16] D. Schubert, J. Richter, F. Jin, K. Michielsen, H. D. Raedt, and R. Steinigeweg, Quantum versus classical dynamics in spin models: Chains, ladders, and square lattices, Phys. Rev. B **104**, 054415 (2021).

[17] A. J. McRoberts, T. Bilitewski, M. Haque, and R. Moessner, Anomalous dynamics and equilibration in the classical Heisenberg chain, Phys. Rev. B **105**, L100403 (2022).

[18] B. Doyon, Lecture notes on Generalised Hydrodynamics, SciPost Phys. Lect. Notes 18 (2020).

[19] S. Blundell, *Magnetism in Condensed Matter*, Oxford Master Series in Condensed Matter Physics (Oxford University Press, Oxford, UK, 2001).

[20] U. Nowak, Classical spin models, in *Handbook of Magnetism and Advanced Magnetic Materials*, edited by H. Kronmüller, S. Parkin, J. E. Miltat, and M. R. Scheinfein (Wiley, Chichester, UK, 2007), pp. 858–876.

[21] R. Rojas, *Neural Networks - A Systematic Introduction* (Springer, Berlin, 1996).

[22] N. G. Berloff, M. Silva, K. Kalinin, A. Askitopoulos, J. D. Töpfer, P. Cilibrizzi, W. Langbein, and P. G. Lagoudakis, Realizing the classical *XY* Hamiltonian in polariton simulators, Nat. Mater. **16**, 1120 (2017).

[23] M. Parto, W. Hayenga, A. Marandi, D. N. Christodoulides, and M. Khajavikhan, Realizing spin Hamiltonians in nanoscale active photonic lattices, Nat. Mater. **19**, 725 (2020).

[24] T. M. Hoang, H. M. Bharath, M. J. Boguslawski, M. Anquez, B. A. Robbins, and M. S. Chapman, Adiabatic quenches and characterization of amplitude excitations in a continuous quantum phase transition, Proc. Natl. Acad. Sci. USA **113**, 9475 (2016).

[25] T. Opatrny, L. Richterek, and M. Opatrny, Analogies of the classical Euler top with a rotor to spin squeezing and quantum phase transitions in a generalized Lipkin-Meshkov-Glick model, Sci. Rep. **8**, 1984 (2018).

[26] A. Cuccoli, A. Taiti, R. Vaia, and P. Verrucchi, Extracting signatures of quantum criticality in the finite-temperature behavior of many-body systems, Phys. Rev. B **76**, 064405 (2007).

[27] A. Caramico D'Auria, L. De Cesare, M. T. Mercaldo, and I. Rabuffo, Quantum-like criticality for a classical transverse Ising model in 4-ϵ dimensions, Eur. Phys. J. B **77**, 419 (2010).

[28] A. Johann, Kink solutions of the classical transverse field Ising chain, Eur. Phys. J. B **25**, 53 (2002).

[29] See Supplemental Material at http://link.aps.org/supplemental/10.1103/PhysRevB.108.L121105 for further technical details.

[30] R. Botet and R. Jullien, Large-size critical behavior of infinitely coordinated systems, Phys. Rev. B **28**, 3955 (1983).

[31] D. Patanè, A. Silva, L. Amico, R. Fazio, and G. E. Santoro, Adiabatic Dynamics in Open Quantum Critical Many-Body Systems, Phys. Rev. Lett. **101**, 175701 (2008).

[32] L. Arceci, S. Barbarino, D. Rossini, and G. E. Santoro, Optimal working point in dissipative quantum annealing, Phys. Rev. B **98**, 064307 (2018).

[33] Y. Bando, Y. Susa, H. Oshiyama, N. Shibata, M. Ohzeki, F. J. Gómez-Ruiz, D. A. Lidar, S. Suzuki, A. del Campo, and H. Nishimori, Probing the universality of topological defect formation in a quantum annealer: Kibble-Zurek mechanism and beyond, Phys. Rev. Res. **2**, 033369 (2020).

[34] M. Kolodrubetz, B. K. Clark, and D. A. Huse, Nonequilibrium Dynamic Critical Scaling of the Quantum Ising Chain, Phys. Rev. Lett. **109**, 015701 (2012).

[35] N. Defenu, T. Enss, M. Kastner, and G. Morigi, Dynamical Critical Scaling of Long-Range Interacting Quantum Magnets, Phys. Rev. Lett. **121**, 240403 (2018).

[36] M. Xue, S. Yin, and L. You, Universal driven critical dynamics across a quantum phase transition in ferromagnetic spinor atomic Bose-Einstein condensates, Phys. Rev. A **98**, 013619 (2018).

[37] O. L. Acevedo, L. Quiroga, F. J. Rodríguez, and N. F. Johnson, New Dynamical Scaling Universality for Quantum Networks Across Adiabatic Quantum Phase Transitions, Phys. Rev. Lett. **112**, 030403 (2014).

[38] T. Caneva, R. Fazio, and G. E. Santoro, Adiabatic quantum dynamics of the Lipkin-Meshkov-Glick model, Phys. Rev. B **78**, 104426 (2008).

[39] A. Chandran, A. Erez, S. S. Gubser, and S. L. Sondhi, Kibble-Zurek problem: Universality and the scaling limit, Phys. Rev. B **86** (6), 064304 (2012).

[40] M.-J. Hwang, R. Puebla, and M. B. Plenio, Quantum Phase Transition and Universal Dynamics in the Rabi Model, Phys. Rev. Lett. **115**, 180404 (2015).

[41] C. De Grandi and A. Polkovnikov, Adiabatic perturbation theory: From Landau–Zener problem to quenching through a quantum critical point, in *Quantum Quenching, Annealing and Computation*, edited by A. K. Chandra, A. Das, and B. K.

Chakrabarti, Lecture Notes in Physics Vol. 802 (Springer, Berlin, 2010).

[42] J. Cardy, *Scaling and Renormalization in Statistical Physics* (Cambridge University Press, Cambridge, UK, 1996).

[43] T. Gao, E. Estrecho, K. Y. Bliokh, T. C. H. Liew, M. D. Fraser, S. Brodbeck, M. Kamp, C. Schneider, S. Höfling, Y. Yamamoto, F. Nori, Y. S. Kivshar *et al.*, Observation of non-Hermitian degeneracies in a chaotic exciton-polariton billiard, Nature (London) **526**, 554 (2015).

[44] I. Rotter and J. P. Bird, A review of progress in the physics of open quantum systems: theory and experiment, Rep. Prog. Phys. **78**, 114001 (2015).

[45] J. M. Zeuner, M. C. Rechtsman, Y. Plotnik, Y. Lumer, S. Nolte, M. S. Rudner, M. Segev, and A. Szameit, Observation of a Topological Transition in the Bulk of a Non-Hermitian System, Phys. Rev. Lett. **115**, 040402 (2015).

[46] L. Feng, Z. J. Wong, R.-M. Ma, Y. Wang, and X. Zhang, Single-mode laser by parity-time symmetry breaking, Science **346**, 972 (2014).

[47] H. Hodaei, A. U. Hassan, S. Wittek, H. Garcia-Gracia, R. El-Ganainy, D. N. Christodoulides, and M. Khajavikhan, Enhanced sensitivity at higher-order exceptional points, Nature (London) **548**, 187 (2017).

[48] E. J. Bergholtz, J. C. Budich, and F. K. Kunst, Exceptional topology of non-Hermitian systems, Rev. Mod. Phys. **93**, 015005 (2021).

[49] Y. Ashida, Z. Gong, and M. Ueda, Non-Hermitian physics, Adv. Phys. **69**, 249 (2020).

[50] R. El-Ganainy, K. G. Makris, M. Khajavikhan, Z. H. Musslimani, S. Rotter, and D. N. Christodoulides, Non-Hermitian physics and PT symmetry, Nat. Phys. **14**, 11 (2018).

[51] M. Fruchart, R. Hanai, P. B. Littlewood, and V. Vitelli, Non-reciprocal phase transitions, Nature (London) **592**, 363 (2021).

[52] A. D. Boozer, Quantum field theory in $(0+1)$ dimensions, Eur. J. Phys. **28**, 729 (2007).

[53] A. Mostafazadeh, Pseudo-Hermiticity versus PT symmetry: The necessary condition for the reality of the spectrum of a non-Hermitian Hamiltonian, J. Math. Phys. **43**, 205 (2002).

[54] A. Mostafazadeh, Exact PT-symmetry is equivalent to Hermiticity, J. Phys. A: Math. Gen. **36**, 7081 (2003).

[55] C. M. Bender, Making sense of non-Hermitian Hamiltonians, Rep. Prog. Phys. **70**, 947 (2007).

[56] W. D. Heiss, The physics of exceptional points, J. Phys. A: Math. Theor. **45**, 444016 (2012).

[57] In principle, the initial condition is $\delta^x(\tau/g) \sim \tau^{-1/3}$ and $\delta^y(\tau/g) \sim \tau^{-2/3} \to 0$ where the latter is taken to zero as it is parametrically smaller than the former in the adiabatic, $\tau \to \infty$ limit.

[58] B. Dóra, M. Heyl, and R. Moessner, The Kibble-Zurek mechanism at exceptional points, Nat. Commun. **10**, 2254 (2019).

[59] L. Xiao, D. Qu, K. Wang, H.-W. Li, J.-Y. Dai, B. Dóra, M. Heyl, R. Moessner, W. Yi, and P. Xue, Non-Hermitian Kibble-Zurek mechanism with tunable complexity in single-photon interferometry, PRX Quantum **2**, 020313 (2021).

[60] E. M. Graefe, H. J. Korsch, and A. E. Niederle, Mean-Field Dynamics of a Non-Hermitian Bose-Hubbard Dimer, Phys. Rev. Lett. **101**, 150408 (2008).

[61] J. W. Van Orden, S. Jeschonnek, and J. Tjon, Scaling of Dirac fermions and the WKB approximation, Phys. Rev. D **72**, 054020 (2005).

[62] Z. Fei, N. Freitas, V. Cavina, H. T. Quan, and M. Esposito, Work Statistics across a Quantum Phase Transition, Phys. Rev. Lett. **124**, 170603 (2020).

[63] T. Puskarov and D. Schuricht, Time evolution during and after finite-time quantum quenches in the transverse-field Ising chain, SciPost Phys. **1**, 003 (2016).

[64] M. Bialonczyk and B. Damski, One-half of the Kibble-Zurek quench followed by free evolution, J. Stat. Mech. (2018) 073105.